A conceptual, distributed snow redistribution model

S. Frey[1] and H. Holzmann[1]

[1]{Institute of Water Management, Hydrology and Hydraulic Engineering, University of Natural Resources and Life Sciences, Vienna, Austria}

Correspondence to: S. Frey (simon.frey@boku.ac.at)

Abstract

When applying conceptual hydrological models using a temperature index approach for snowmelt to high alpine areas often accumulation of snow during several years can be observed. Some of the reasons why these “snow towers” do not exist in nature are vertical and lateral transport processes. While snow transport models have been developed using grid cell sizes of tens to hundreds of square meters and have been applied in several catchments, no model exists using coarser cell sizes of one km², which is a common resolution for mean and large scale hydrologic modelling. In this paper we present an approach that uses only gravity and snow density as a proxy for the age of the snow cover and land-use information to redistribute snow in Alpine basins. The results are based on the hydrological modelling of the Austrian Inn basin in Tyrol, the detailed description of the current paper refer to the catchment of Ötztaler Ache, Austria, but the findings hold for other tributaries of the river Inn. This transport model is implemented in the distributed rainfall-runoff model COSERO. A comparison for model validation between the standard model without parameterization for lateral snow redistribution and the updated version is done using observed discharge and MODIS derived snow covered areas. While the signal of snow redistribution can hardly be seen in the binary classification compared with MODIS, snow accumulation over several years can be prevented. In a seven year period the standard model would lead to snow accumulation of approximately 2900 mm SWE in high elevated regions whereas the updated version of the model does not show accumulation and does also predict discharge more precisely leading to a Kling-Gupta-Efficiency of 0.93 instead of 0.9. A further improvement can be shown in the comparison of MODIS snow cover data and the calculated depletion curve, where the redistribution model increased the efficiency (R^2) from 0,70 to 0,78 (calibration) and from 0,66 to 0,74 (validation).

1 Introduction

Conceptual models are widely used in hydrology. Examples are the HBV model (Bergström, 1976), PDM (Moore, 2007), GSM-SOCONT (Schaefli et al., 2005) or VIC (Wood et al., 1992) just to name a few. Many of these conceptual models use a temperature index approach to model snow melt and snow accumulation and even in some physically based models as e. g. versions of the SHE model (Bøggild et al., 1999) this method can be found. This approach has the advantage of being quite simple since it uses only temperature as input to determine whether precipitation occurs in the form of snow or rain and whether snow can be melted or not. A typical example of a temperature index method for snow modelling is the degree-day approach (see for example Hock 2003). A disadvantage is that snow accumulates as long as the air temperature does not rise above a certain threshold (often 0 °C) regardless of any other processes that may lead to snow melt like radiation or turbulent fluxes of latent energy. In high mountainous areas this may be the case for most days in the year leading to an intensive computational accumulation of snow in these areas. In the modellers terminology these artefacts are often called "snow towers". In nature, however, these accumulations are barley existent.

The reasons for that are either wind or gravitationally induced lateral snow distribution processes (Elder et al., 1991; Winstral et al., 2002). Resulting snow depths are not uniformly distributed in space but vary within large ranges (Helfricht et al., 2014). When changing the focus from micro (e. g. several square meters) to macro scales (e. g. one to several square kilometres), variations become less (Melvold and Skaugen, 2013). The intention of the applied snow redistribution concept was (a) to prevent the artefacts of "snow towers" and (2) to develop a concept which considers gravity driven lateral snow transport with reasonable and plausible process depiction.

1.1 Theoretical background of snow cover variations

During the accumulation period, according to Liston (2004), primarily three mechanisms are responsible for these variations: (i) snow-canopy interactions in forest covered regions, (ii) wind induced snow redistribution and (iii) orographic influences on snow fall. These mechanisms influence snow cover patterns on scales ranging from the micro to the macro scale. Spatial snow cover variability beneath canopies is mainly affected by different tree species (deciduous vs coniferous trees) influencing LAI, height and density of the canopy and gap sizes (Garvelmann et al., 2013; Liston, 2004; Pomeroy et al., 2002).

Besides the impact of vegetation, wind is the most dominant factor influencing snow patterns in alpine terrain. Snow is transported from exposed ridges to the lee side of these ridges, valleys and vegetation covered areas (Essery et al., 1999; Liston and Sturm, 1998; Rutter et al., 2009; Winstral et al., 2002). One has to be aware that besides of the physical transport of solid snow wind also stimulates sublimation processes (Liston and Sturm, 1998; Strasser et al., 2008). Wind influences snow depth distributions on scales of some 100s to 1000 square metres (Dadic et al., 2010a).

The third mechanism (orographic effect) influences snow patterns on a larger scale of one to several kilometres (e. g. Barros and Lettenmaier, 1994). Non-uniform snow distributions are caused by interactions of the atmosphere (air pressure, humidity, atmospheric stability) with topography (Liston, 2004).

In addition to these processes, avalanches play a role in snow redistribution (Lehning and Fierz, 2008; Lehning et al., 2002; Sovilla et al., 2010). In steep terrain, avalanches depend mainly on the slope angle and are capable of transporting large snow masses over distances of tens to hundreds of metres (Dadic et al., 2010b; Sovilla et al., 2010).

During the ablation period, spatial snow distributions are mainly influenced by differences in snow melt behaviour. On the northern hemisphere, on south-facing slopes, rates of snow melt are generally enhanced compared to north-facing slopes due to the inclination of radiation. Also vegetation influences melting behaviour. Shading reduces snowmelt compared to direct sunlight. Enhanced emitted long wave radiation due to warm bare rocks or trees increases the melt rate (Garvelmann et al., 2013; Pohl et al., 2014).

1.2 Modelling approaches

A common approach avoiding intensive accumulation of snow is editing the meteorological input (Dettinger et al., 2004). For instance, many models use a constant yet adjustable lapse rate for interpolating temperature with elevation (Holzmann et al., 2010; Koboltschnig et al., 2008). Besides temperature, precipitation gradients are often adjusted to fit observed and modelled target variables (e. g. snow patterns or runoff) (Huss et al., 2009b; Schöber et al., 2014). Justification for doing so is the general lack of gauging stations in the summit regions (Daly et al., 1994, 2008) along with the high error of precipitation gauges (Rasmussen et al., 2011; Williams et al., 1998). An approach presented by Jackson (1994) defining a precipitation correction matrix was successfully applied in several studies (Farinotti et al., 2010; Huss et al., 2009a). Scipión et al. (2013) however identified significant discrepancies between precipitation patterns obtained by a Doppler X-band radar and the snow accumulation at the end of the winter period which gives clear indications that snowfall is redistributed based on different driving forces. Consequently, the variability of the meteorological input cannot explain the variability of snow cover patterns.

Models trying to deal with snow accumulation and redistribution apart from input corrections may be classified into two major approaches. One is the consideration of process based snow distribution patterns the other approach is empirical. Examples for process oriented model are SNOWPACK (Bartelt and Lehning, 2002) used in avalanche research or SnowTran3D (Liston et al., 2007; Liston and Sturm, 1998). Empirical models use the fact, that snow patterns resemble each other every year (Helfricht et al., 2012, 2014). The presented paper concentrates on the empirical approach.

Helfricht et al. (2012) used airborne LiDAR measurements to determine snow accumulation gradients for elevation bands in the Ötztaler Alps. These could be used to improve hydrological models regarding snow cover distributions and subsequently to achieve better runoff predictions. LiDAR data, however, are relatively expensive. Often wind speed and -direction are used to model snow drift (e.g. Bernhardt et al., 2009; 2010; Shulski and Seeley, 2004; Winstral et al., 2002; Liston and Sturm, 1998). Kirchner et al. (2014) concluded from LiDAR measurements in combination with meteorological stations in a catchment in California, USA that wind measurements from only one meteorological station are of too poor quality for a useful description of wind fields for snow transport. The computed wind fields generated by regional circulation models (RCM) have also shown to be erroneous (Nikulin et al., 2011) and therefore are not useful for direct implementation in redistribution models. Additionally models using wind have in common that they are computationally intensive as they require data in high spatial resolution (e. g. 100 to 1000s of square metres). Schöber et al. (2014) combined gravitational and wind induced snow transport using a distributed energy balance model with a resolution of 50x50 m.

However, the difficulties of snow accumulation also occur when models with coarser cell sizes are applied. Due to some available databases for vegetation and meteorology (Haiden et al., 2011; Masson et al., 2003; Oubeidillah et al., 2014), many models operate on cell sizes of

1 km² or more (e. g. Andersen et al., 2001; Henriksen et al., 2003; Mauser and Bach, 2009; Safeeq et al., 2014). To our knowledge, no model for redistributing snow on a 1x1 km grid size exists. In this paper we present a simple approach to deal with snow in high mountainous regions and its application in the catchment of Ötztaler Ache in Tyrol, Austria. Since the model uses meteorological input from INCA (Haiden et al., 2011) that already account for meteorological corrections, we focus on snow redistribution rather than to edit the input data. As already mentioned the two main objectives in this respect are to achieve a better model efficiency regarding runoff and to avoid the existence of snow towers at high altitudes.

2 Model description

2.1 Hydrological Model COSERO

COSERO is a spatially distributed conceptual hydrological model which is similar to the HBV model (Bergström, 1976). In the presented paper it uses 1x1 km grid cells. Originally developed for modelling discharge of the Austrian rivers Enns and Steyer (Nachtnebel et al., 1993), it has recently been used for different purposes like climate change studies (e. g. Kling et al., 2012, 2014b; Stanzel and Nachtnebel, 2010), investigating the role of evapotranspiration in high alpine regions (Herrnegger et al., 2012) and operational runoff forecasting (Stanzel et al., 2008). Potential evapotranspiration is calculated using the Thornthwaite method (Thornthwaite, 1948). Discharge due to rainfall and snow-/ice melt is estimated using the same non-linear function of soil moisture as the original HBV. In this study, the model is run using daily time steps. It is, however, capable of using hourly or monthly time steps. In the latter case, intra-monthly variations are considered for snow and interception processes as well as for soil moisture (Kling et al., 2014a). A schematic overview of the model is given by Fig. 1 and a detailed description of the model can be found in Kling et al. (2014a), where the model was applied to several catchments across Europe, Africa and Australia. However, in Kling et al. (2014a) snow parameters were not calibrated and therefore the snow module is not fully explained in detail in their paper. This will be done in the following. Equations (1) to (7) and (10) were taken from the original model by Stanzel and Nachtnebel (2010), all other methods were developed in the present study.

Numerous studies have shown that sub-grid variability of snow depths can be described by a two parameter log-normal distribution (e. g. Donald et al., 1995; Pomeroy et al., 1998).

COSERO uses five snow classes per cell (i.e. the log-normal distribution is subdivided into five quantiles) to approximate this sub-grid log-normal distribution under accumulation conditions (see Fig. 2 b)), i. e. snowfall is distributed log-normally into snow classes, where the sum of the snow water equivalent (SWE) of each classes represent the mean conditions in the grid cell. This distribution can be interpreted as a statistical description of snow distribution processes taking place at the subgrid scale (Pomeroy et al., 1998). This method has the potential to indirectly consider the influence of curvature, shelter, vegetation or elevation (Hiemstra et al., 2006). The properties of each class are treated unique as equations (1) to (13) apply to every snow class separately. Consequently the log-normal distribution within a grid cell may be disturbed by the processes of melting, sublimation, refreezing and redistribution to other grid cells. Once fallen, snow redistribution between the snow classes within a single grid cell is not considered. A scheme of the composition of a snow class is illustrated in Fig. 2 a). The snow water equivalent (S_{SWEt}) of a given day t per class is calculated by Eq. (1) where P_{Rt} and P_{St} are liquid and solid precipitation in mm, respectively, M_t is snow melt and E_{St} is sublimation of snow. All variables are given in mm SWE.

$$S_{SWE_t} = S_{SWE_{t-1}} + P_{R_t} + P_{S_t} - M_t - E_{S_t} \tag{1}$$

Snow melt is calculated by a temperature index approach (see for example Hock 2003). Eq. (2) is used:

$$M_t = min\left(S_{SWE_t}; P_{R_t} \cdot \varepsilon \cdot T_{AIR_t} + D_{f_t} \cdot T_{AIR_t}\right) \tag{2}$$

where M_t is snowmelt [mm], ε is the ratio of specific heat of water and melting energy, T_{AIRt} is the (mean) daily air temperature [°C] and D_{ft} [mm °C^{-1}] is the snow melt factor of a given day t estimated by Eq. (3):

$$D_{f_t} = \left(-cos\left(J \cdot \frac{2\pi}{365}\right) \cdot \frac{D_U - D_L}{2} + \frac{D_U - D_L}{2}\right) \cdot M_{RED_t} \tag{3}$$

with

$$M_{RED_t} = \begin{cases} D_{RED}, & S_{fresh} \geq S_{CRIT} \\ M_{RED_{t-1}} + \frac{(1 - M_{RED_{t-1}})}{5}, & S_{fresh} < S_{CRIT} \end{cases} \tag{4}$$

where J is the Julian day of the year [-], D_U and D_L are the upper and lower boundaries of D_f [mm °C^{-1}], respectively, and M_{RED} [-] is a reduction factor to account for the higher albedo caused by freshly fallen snow calculated by Eq. (4). S_{CRIT} [mm] is the critical snow depth of fresh snow necessary to increase the albedo, whereas S_{fresh} is the actual depth of fresh snow

[mm] fallen within one time step. For fresh snow depth larger than S_{CRIT}, M_{RED} is set to a reduced melting factor D_{RED} [-].

Whether precipitation occurs in form of snow or rain is controlled by two parameters T_{PS} and T_{PR}, defining the temperature range where snow and rain occur simultaneously. At and above temperature T_{RP} precipitation is pure liquid, at and below T_{PS} precipitation is pure solid. In between those two boundaries, the proportion of solid to liquid precipitation is estimated linearly.

For the estimation of snow sublimation, Eq. (5) is used, where E_{SP} [mm] refers to potential sublimation of snow, E_P [mm] is the potential evapotranspiration and E_R is a correction factor to reduce E_P. Sublimation is considered only for snow classes actually covered by snow. Hence, if a grid cell is partly snow free (this can be the case if one subgrid class has no snow cover due to melting) sublimation is estimated for the snow covered part only. For the uncovered classes evapotranspiration according to the Thornthwaite method is applied.

$$E_{SP_t} = E_{P_t} \cdot E_R \qquad (5)$$

The snow cover in COSERO is treated as porous medium and therefore is able to store a certain amount of liquid water (S_l) in dependency of the snow pack density (ρ) calculated using Eq. (6).

$$S_{l_t} = \left(S_{SWE_t} - S_{l_{t-1}}\right) \cdot \left(S_{lMAX} - (\rho - \rho_{MAX}) \cdot S_{l\rho}\right) \qquad (6)$$

Where S_{lMAX} [$m^3\ kg^{-1}$] is the maximum water holding capacity at the maximum snow density of the snow pack ρ_{MAX} [$kg\ m^{-3}$] and $S_{l\rho}$ describes the decrease of water holding capacity with increasing snow density ρ.

At negative air temperatures, retained melt water has the ability to refreeze in the snow pack. The potential amount of refrozen water (S_R) is estimated by Eq. (7), where R_f is the refreezing factor [mm °C^{-1}]. As long as there is enough liquid water in the snow pack, actual refreezing will be equal to potential refreezing.

$$S_R = \begin{cases} 0, & T_{AIR_t} > 0 \\ R_f \cdot \left(T_{AIR_t} \cdot (-1)\right), & T_{AIR_t} \leq 0 \end{cases} \qquad (7)$$

Refrozen water is treated in the same way as snow. The amount of water leaving the snow cover then equals snowmelt minus retained water.

Snow density (ρ_t) of each class is calculated using a sigmoid function shown in Eqs. (8) and (9) where ρ_{MAX} and ρ_{MIN} are the respective maximum and minimum values of ρ, T_{AIR} is the temperature of the air mass above the snow layer and ρ_{scale} and T_{scale} are scaling coefficients to calculate a transition temperature (T_{tr}) for the estimation of the snow density. Herby, ρ_{scale} adjusts the slope of the function, whereas T_{scale} is responsible for a shift on the x-axis. These two parameters are set to fixed values of 1.2 and 1, respectively. The solution of Eqs. (8) and (9) is illustrated in Fig. 3 for a range of typical air temperatures, where snowfall occurs. Already fallen snow can reach a higher density (ρ_{OLD}) than fresh snow. Its density is calculated using a time settling constant (ρ_{SET}, derived from Riley et al., 1973) until the maximum density is reached (Eq. 10).

$$\rho_t = (\rho_{MAX} - \rho_{MIN}) \cdot \left(\frac{T_{tr}}{\sqrt{1+(T_{tr})^2}} + 1\right) \cdot 0.5 + \rho_{MIN} \tag{8}$$

with

$$T_{tr} = \frac{T_{AIR_t}}{\rho_{scale}} + T_{scale} \tag{9}$$

$$\rho_{OLD} = \frac{\rho_{SET} \cdot \left(\frac{SSWE_t}{\rho_{OLD}} + \frac{S_t}{2}\right)}{1 + \frac{\rho_{SET}}{2}} \tag{10}$$

The COSERO model considers both snow and glacier ice melt processes. Ice melt (M_{ICE}) is computed by means of a degree-day method (see Eq. 11) and uses separate parameter sets. Here, D_{ICE} refers to the ice melt factor [mm °C^{-1}]. A prerequisite of ice melt is the full depletion of the overlying snow cover. Spatial information of glaciers are taken from the Randolph Glacier Inventory version 3.2 (Arendt et al., 2012).

$$M_{ICE} = D_{ICE} \cdot T_{AIR} \tag{11}$$

2.2 Snow transport model

Several authors reported that the slope angle has an important influence on snow depths (Bernhardt and Schulz, 2010; Kirchner et al., 2014; Schöber et al., 2014). The model redistributes snow only to grid cells providing the steepest slope (acceptor cell) in the direct neighbourhood of the raster cell it searches from (donor cell). Only downward transportation is considered. If more than one cell show the same (largest) difference in elevation, the amount of donated snow is distributed equally to the number of acceptor cells. The actual amount of snow being redistributed depends on the steepness of the slope, the age of the snow cover, considered by the density of snow, the type of land cover of the donor cell and the snow depth of the donor cell. The drier (less dense) the snow pack the higher the snow rate available for the redistribution routine (f_ρ, Eq. 13). Thus the defined maximum density of snow (450 kg m^{-3}) determines the threshold for snow redistribution. The availability of snow for transport is determined by a vegetation-based threshold value (H_v) for each class of land cover. This value can also be interpreted as a roughness coefficient for areas where no or hardly any vegetation is present like in alpine and nival elevations. If the snow depth (S [mm]) of a snow class of a raster cell exceeds H_v [mm], snow transport from that cell is activated and redistribution is calculated by solving Eqs. (12) and (13).

$$= max(S_D - H_v; 0) \cdot f_\rho \cdot \frac{1}{\sum A} \cdot C \qquad (12)$$

With

$$f_\rho = \left(\frac{(\rho_{MAX} - \rho_D)}{\rho_{MAX}} \cdot e^{\left(-\frac{\rho_D}{\rho_{MAX}}\right)} \right) \cdot \frac{\alpha}{90} \qquad (13)$$

Where $S_{SWE(A)}$ is the amount of snow water equivalent that is redistributed from the donor cell (D) to the available acceptor cell(s) (A), ρ_D is the density of snow in the donor cell, ρ_{MAX} is the possible maximum density of snow, α is the angle of the slope between the donor and acceptor cells in degree and C is a correction coefficient that can be calibrated.

Notwithstanding, that other geomorphological properties than slope angle influencing snow patterns are important on scales smaller than the grid size of COSERO (see section 1.1), slope was selected as driving force for the model. One has to be aware that this is a simplification and under realistic conditions snow might not necessarily be transported only on the steepest route (Bernhardt and Schulz, 2010; Winstral et al., 2002).

Fig. 4 illustrates the shape of the distribution coefficient f_p as a function of different elevation gradients between the acceptor and donor cells and of the snow density. In acceptor cells redistributed snow is treated as fresh snow in the sense that it is distributed to the snow classes according to the log-normal distribution.

The model is organized in form of a loop starting at the highest grid cell (summit region) and ending at the lowest cell (outlet of the catchment). This ensures that snow cannot be redistributed into already processed grid cells. Snow will be transported downslope as long as the slope is big enough to allow for transportation given that the density of snow is low enough. Consequently, snow accumulates rather in flat regions of the catchment. The concept of the redistribution model is sketched in Fig. 5. Note that although snow depths in the highest cell are prevented by the model, the number of snow covered cells remains the same.

3 Case study in the catchment the Ötztaler Ache, Tyrol, Austria

3.1 Catchment description

The catchment of Ötztaler Ache at gauge Huben, situated in western Austria close to the Italian border, covers an area of 511 km² and has an altitudinal range between 1185 m a.s.l at the gauge at Huben and 3770 m a.s.l at its highest peaks. Due to the use of a 1x1 km gridded DEM, the highest grid cell has a mean elevation of 3450 m a.s.l, whereas the lowest cell has an elevation of 1250 m a.s.l. (Fig. 6). About 30 % of its area is covered by vegetation, mainly pastures and meadows. Glaciers cover about 19 % leading to an annual ice melt contribution of about 25 % of the total runoff at Huben, while 41 % of the discharge has its origin in snowmelt (Weber et al., 2010). Table 1 gives an overview of the land cover.

In Fig. 6 the elevations of the Ötztal basin are described. Frequency distribution of slope angles derived from 1x1 km grid are shown (6 a). This frequency distribution exhibits the highest frequencies in the slope classes between 20 and 25 degrees for higher elevations. In lower elevated regions slope classes between 0 and 15 degrees dominate. However, also glacier covered areas at the summits can have flat slopes. Note that the listed slopes are based on the steepest vertical gradients of the neighbour elements.

3.2 Input data

Gridded meteorological data of precipitation and air temperature are required to run the model. These data are provided by the INCA dataset (Haiden et al., 2011) with the same grid spacing like the hydrological model, allowing a direct use in the model without the need for pre-processing. INCA data are available since 2003. The years 2003 and 2004 have been used as a warm-up period for the model. In the subsequent years no correction of meteorological data was done since INCA already accounts for elevation gradients regarding air temperature and precipitation. Six land use classes were derived from the most recent CORINE data set (CLC2006 version 17, see EEA, 1995). These classes and their areal fractions in the catchment of Ötztaler Ache are given in Table 1. It should be pointed out, that neither radiation nor wind speed or wind direction data are necessary to run the model.

3.3 Model calibration

The hydrological model was calibrated for the period from 2005 to 2008 using a Rosenbrock's automated optimization routine (Rosenbrock, 1960). Although the model is rich of parameters, the vast majority of them have been estimated *a priori* according to literature (Liston and Sturm, 1998; Prasad et al., 2001) and previous work on the model (Fuchs, 2005; Kling, 2006; Nachtnebel et al., 2009). In the snow model including snow redistribution only six parameters have been calibrated: upper and lower boundaries of snow melt factors D_U and D_L, respectively, the threshold values that control the range where liquid and solid precipitation occur simultaneously (T_{PR}, T_{PS}), the standard deviation of the log-normal distribution of snow depth in one grid cell (N_{VAR}) and the calibration parameter for snow redistribution C (see Eq. 12). The limited number of optimization parameters reduces equifinality problems. For a more detailed description of equifinality issues see the supplements of this article. The target of the calibration was a good fit of runoff using the Kling-Gupta-Model-Efficiency (Gupta et al., 2009; Kling et al., 2012) as objective function. The model was validated for the years 2009 and 2010. Both calibration and validation have been done with and without using the snow drift module. In the following model A refers to the model using snow transport, whereas model B stands for the standard model. Vegetation threshold values for snow detention were taken from previous studies (Liston and Sturm, 1998; Prasad et al., 2001). These are given in Table 1. Maximum snow density was assumed 450 kg m^{-3} which matches long term snow measurements (Jonas et al., 2009; Schöber et al., 2014).Besides discharge in the validation period also snow cover data from MODIS (8 day maximum snow cover, version 5) satellite images (Hall et al., 2002) were used to compare the performance of both models.

4 Results

4.1 Discharge

Fig. 7 shows a comparison of total discharge using model A and B at the gauge Huben for the year 2006. Both models result in similar quality criteria in the calibration as well as in the validation period (see Table 2). Nevertheless, the model efficiency could be improved by 0.05 in the calibration period and 0.02 in the validation period by accounting for lateral snow transport. Maximum differences in the mean daily discharges between the two models reach up to 2 mm per day (which equals to 12.1 $m^3 s^{-1}$) leading to a relative difference of minus 9 up to 44 % of model A in respect to model B. In total, model A generates a surplus of about 300 mm discharge in five years compared to model B (Fig. 8). About 2/3 of the additional discharge originate in enhanced snowmelt the rest occurs due to enhanced glacier melt.

4.2 Spatially distributed snow cover data

Fig. 9 compares model A and B with MODIS snow depletion data. Both the accumulation period in winter and the ablation period in spring and summer are represented well by both models. Cold snowfall periods in summer generate sharp peaks in the depletion curve, which could be calculated by both model versions, where Model A computed slightly smaller peaks during the snowmelt period (May to July). This leads to a moderate increase of the determination factor R^2 from 0.70 to 0.78 (calibration) and from 0.66 to 0.74 (validation).

4.3 Inter annual snow accumulation

The main reason for developing a snow transport model was the prevention of “snow towers” – accumulation of snow over several years in high mountainous regions. Fig. 10 presents model behaviour of model A and B with respect to the accumulation of snow in elevations above 2800 m a.s.l. This elevation was chosen because here none of the models indicates snow accumulation for more than one year and therefore snow accumulation in lower altitudes is no problem. By the end of seven years of modelling, model B shows snow depths of approx. 2900 mm SWE in elevations above 3400 m a.s.l. whereas model A does hardly show any accumulation behaviour in these altitudes. Spatially distributed net loss and gain of snow for all raster cells within the period of one year in the watershed are presented in Fig. 11. It can be shown that net loss is evident in the zones of ridges and high elevations, where the maximum net gain is along the valley bottoms.

4.4 Parameter equifinality

Since the model uses several parameters that need calibration it suffers from equifinality issues. To investigate those issues, Monte Carlo simulations have been carried out varying the snow relevant parameters that cannot be estimated a priori. Since the aim of this paper is snow transport, the results of the Monte Carlo simulations can be found in the supplements of this article.

5 Discussion

5.1 Discharge

In spring, at the beginning of the melting season, higher runoff is generated by model A due to a larger amount of snow in lower altitudes (see Fig. 7). Later in the year enhanced glacier melt is mainly responsible for higher discharge rates. About 200 mm have their origin in enhanced snowmelt, while the remaining 100 mm originate in amplified melt of glaciers. Since glacier cover about 19.4 % of the catchment's area 100 mm of additional mean basin runoff corresponds to an enhanced negative glacier mass balance of -500 mm. The reason for this is transport of snow in warmer altitudes and therefore earlier and more snow free glacier surfaces producing higher discharge due to glacier melt (see Fig. 8) and explains the peak in July and August in runoff difference (see Fig 7).

5.2 Spatially distributed snow cover data

Fig. 9 shows the snow depletion curve of the year 2009 based on MODIS data and the comparison of model runs A and B. Only little differences between model A and B can be identified. The reason for this is the vegetation threshold. Even if snow is being transported, a residual of snow remains in the donor cell resulting in the cell marked as snow covered. Grid cells covering the summits only donate snow to their respective acceptor cells. However, a certain amount of snow is held back according to the threshold due to vegetation and roughness of the surface. As indicated in Fig. 5 grid cells nested in the intermediate slope regions receive and donate snow at the same time. Thus their snow depth changes little if comparing model A and model B. In flat valley regions, grid cells only receive snow, where relatively high air temperature values often allow for melting.

Satellite based snow cover information by MODIS are binary and so is the model output for comparing these results. In a binary system, no difference can be distinguished between cells covered by much or little snow.

5.3 Snow accumulation

While using model B, the higher the elevation the more snow is accumulated. Contrary, model A shows less pronounced and in some high altitudes even contrary behavior(see Fig.

10). This is a result of the slope dependency of the distribution model that the amount of snow distributed to other grid cells is higher with increasing vertical distance to the downward grid cell. In general and in the Ötztal as well mountains are steeper in the summit regions than at the bottom (see Fig. 6). Consequently in the summit regions snow will be preferentially eroded while it accumulates at the rather flat valleys where the vertical distances between the grid cells are less than at the peaks. This does reflect snow accumulations that can be observed in nature where summits might be nearly snow free in spring while flatter parts are still covered with snow. While the raster cells covering peak regions act as donators only those cells located on slopes may receive and distribute snow at the same time (Fig. 11). Valley regions only receive snow. The resulting net loss and gain areas shown in Fig. 11 give some indication that the redistribution algorithm is plausible.

Although snow accumulation behaviour of model A is more realistic than model B snow accumulation can still be observed in the highest elevations zone (see Fig. 10). This is based on the parameterization of the snow holding capacity Hv, where even bare ground assigns a value of 200 mm (see Table 1). The influence of the highest elevation class (> 3400 m a.s.l.) on both the hydrograph and snow covered area however is very small, since this elevation level is represented by only four grid cells. Consequently the objective function during calibration using an automated optimization routine like Rosenbook's routine does not differ much when underestimating the correction coefficient in these grid cells.

The smaller the portion of high altitude areas in a catchment compared to the total catchment area the less important is snow redistribution for modelling runoff. This ratio of summit regions to total catchment size is normally smaller for bigger catchments. The catchment of river Inn, for instance, covers an area of about 10000 km² yet only 733 km² are located at elevations where intensive snow accumulations and mobilizations occur (above 2800 m a.s.l.). In the Ötztal basin 204 out of 511 km² are located higher than 2800 m a.s.l. If model A is applied to the catchment of river Inn in five years of modelling about 15 mm SWE (with respect to the entire river basin) remain in the catchment due to snow accumulation processes instead of 300 mm in the Ötztal.

5.4 Transferability to other catchments

The model provides results that have been found by other models, too. For instance the elevation where the highest snow accumulations occurs (2800 to 3000 m a.s.) as was found by

LiDAR measurements in the same catchment (Helfricht et al., 2012) as well as by modelling (Frey, 2015). Given that and the needs of the model (slope angles, snow density) for transporting snow, it produces valid results as long as a catchment features relatively steep slopes in the summit regions (which is the case in most catchments in the Alps). Obviously, the model needs calibration if it is transferred to another catchment.

5.4 Parameter equifinality

Like most hydrological models COSERO requires calibration of some parameters. This necessarily causes equifinality issues (Beven and Freer, 2001). The more adjustable parameters a model provides, the more important this problem may become (e. g. Gupta et al., 2008). On the other hand, some authors pointed out that more complex models may produce more feasible results if the parameters can be estimated within realistic boundaries (Gharari et al., 2012, 2014; Hrachowitz et al., 2014). Applying COSERO with the presented snow redistribution routine requires two additional parameters: the vegetation threshold H_V (estimated *a priori*) and the calibration parameter C (see Eq. 12). Yet, accounting for snow redistribution allows the modeller to use D_U values within or close to the range proposed by Kling et al., (2006), while the standard version of the model leads to the best results if higher and therefore unrealistic D_U values are used (see supplements of this article).

6 Conclusions

A model for redistribution of snow on a coarse 1x1 km raster has been developed and tested in the catchment of Ötztaler Ache, Austria. While only little improvement of snow cover compared to MODIS data could be achieved, appearance of “snow towers” in high altitudes could be prevented. In terms of discharge at the outlet of the basin, both models show good results. However, the Kling-Gupta-efficiency of model A could be improved by 0.05 in the calibration and by 0.02 in the validation period. With respect to the entire watershed area the model using snow redistribution generates about 200 mm more runoff originated from snowmelt in five years than without considering this process. This does not only affect the water balance of the catchment but also amplifies glacier melt about 500 mm in five years, with respect to glaciated areas, due to longer time periods where glacier surfaces are fully snow free.

The integration of a snow transport module promotes the demand, that models work “right for the right reasons” and is an attempt to integrate more real process understanding into the model approach. Further work needs to be carried out with respect to validation of spatially distributed snow patterns. For this purpose, satellite images from Landsat might be of use providing a higher spatial resolution than MODIS.

Even though the vast majority of parameters were estimated *a priori* in this work, equifinality remains an issue. However, redistribution of snow requires only two additional parameters but allows for more realistic boundaries (see Kling et al., 2006) of the snow melt factors (see supplements of this article). However, more work needs to be carried out to account for that issue.

Acknowledgements

The authors thank their colleagues for continuing support and discussion around the coffee breaks, especially to Matthias Bernhardt for friendly reviewing and commenting on the manuscript. Special thanks to Herbert Formayer and David Leidinger of the institute of meteorology, BOKU, for supplying the INCA data. Many thanks to Daphné Freudiger and two further anonymous referees for their comments and valuable suggestions. This study was part of a research project in cooperation with Verbund AG.

References

Andersen, J., Refsgaard, J. C. and Jensen, K. H.: Distributed hydrological modelling of the Senegal River Basin — model construction and validation, J. Hydrol., 247(3-4), 200–214, doi:10.1016/S0022-1694(01)00384-5, 2001.

Arendt, A., Bolch, T., Cogley, J. G., Gardner, A., Hagen, J.-O., Hock, R., Kaser, G., Pfeffer, W. T., Moholdt, G., Paul, F., Radić, V., Andreassen, L., Bajracharya, S., Barrand, N., Beedle, M., Berthier, E., Bhambri, R., Bliss, A., Brown, I., Burgess, D., Burgess, E., Cawkwell, F., Chinn, T., Copland, L., Davies, B., De Angelis, H., Dolgova, E., Filbert, K., Forester, R. R., Fountain, A., Frey, H., Giffen, B., Glasser, N., Gurney, S., Hagg, W., D., H., Haritashya, U. K., Hartmann, G., Helm, C., Herreid, S., Howat, I., Kapusti, G. G., Khromova, T., Kienholz, C., Köonig, M., Kohler, J., Kriegel, D., Kutuzov, S., Lavrentiev, I., Le Bris, R., Lund, J., Manley, W., Mayer, C., Miles, E., Li, X., Menounos, B., Mercer, A., Mölg, N., Mool, P., Nosenko, G., Negrete, A., Nuth, C., Pettersson, R., Racoviteanu, A., Ranzi, R., Rastner, P., Rau, F., Raup, B., Rich, J., Rott, H., Schneider, C., Seliverstov, Y., Sharp, M., Siguosson, O., Stokes, C., Wheate, R., Winsvold, S., Wolken, G., Wyatt, F. and Zheltyhina, N.: Randolph Glacier Inventory - A Dataset of Global Outliners: Version 3.2, Boulder Colorado, USA., 2012.

Barros, A. P. and Lettenmaier, D. P.: Dynamic modeling of orographically induced precipitation, Rev. Geophys., 32(3), 265, doi:10.1029/94RG00625, 1994.

Bartelt, P. and Lehning, M.: A physical SNOATACK model for the Swiss avalanche warning Part I: numerical model, Cold Reg. Sci. Technol., 35(3), 123–145, doi:10.1016/S0165-232X(02)00074-5, 2002.

Bergström, S.: Development and application of a conceptual runoff model for Scandinavian catchments, SMHI Reports RHO, No. 7, Norrköping, 1976.

Bernhardt, M., Liston, G. E., Strasser, U., Zängl, G. and Schulz, K.: High resolution modelling of snow transport in complex terrain using downscaled MM5 wind fields, Cryosph., 4(1), 99–113, doi:10.5194/tc-4-99-2010, 2010.

Bernhardt, M. and Schulz, K.: SnowSlide: A simple routine for calculating gravitational snow transport, Geophys. Res. Lett., 37(11), L11502, doi:10.1029/2010GL043086, 2010.

Bernhardt, M., Zängl, G., Liston, G. E., Strasser, U. and Mauser, W.: Using wind fields from a high-resolution atmospheric model for simulating snow dynamics in mountainous terrain, Hydrol. Process., 23(7), 1064–1075, doi:10.1002/hyp.7208, 2009.

Beven, K. and Freer, J.: Equifinality, data assimilation, and uncertainty estimation in mechanistic modelling of complex environmental systems using the GLUE methodology, J. Hydrol., 249, 11–29, doi:10.1016/S0022-1694(01)00421-8, 2001.

Bøggild, C. E., Knudby, C. J., Knudsen, M. B. and Starzer, W.: Snowmelt and runoff modelling of an Arctic hydrological basin in west Greenland, Hydrol. Process., 13(12-13), 1989–2002, doi:10.1002/(SICI)1099-1085(199909)13:12/13<1989::AID-HYP848>3.0.CO;2-Y, 1999.

Dadic, R., Mott, R., Lehning, M. and Burlando, P.: Parameterization for wind-induced preferential deposition of snow, Hydrol. Process., 24(June), 1994–2006, doi:10.1002/hyp.7776, 2010a.

Dadic, R., Mott, R., Lehning, M. and Burlando, P.: Wind influence on snow depth distribution and accumulation over glaciers, J. Geophys. Res. Earth Surf., 115(1), F01012, doi:10.1029/2009JF001261, 2010b.

Daly, C., Halbleib, M., Smith, J. I., Gibson, W. P., Doggett, M. K., Taylor, G. H., Curtis, J. and Pasteris, P. P.: Physiographically sensitive mapping of climatological temperature and precipitation across the conterminous United States, Int. J. Climatol., 28, 2031–2064, doi:10.1002/joc.1688, 2008.

Daly, C., Neilson, R. P. and Phillips, D. L.: A Statistical-Topographic Model for Mapping Climatological Precipitation over Mountainous Terrain, J. Appl. Meteorol., 33, 140–158, doi:10.1175/1520-0450(1994)033<0140:ASTMFM>2.0.CO;2, 1994.

Dettinger, M., Redmond, K. and Cayan, D.: Winter Orographic Precipitation Ratios in the Sierra Nevada—Large-Scale Atmospheric Circulations and Hydrologic Consequences, J. Hydrometeorol., 5(1992), 1102–1116, doi:10.1175/JHM-390.1, 2004.

Donald, J. R., Soulis, E. D., Kouwen, N. and Pietroniro, A.: A Land Cover-Based Snow Cover Representation for Distributed Hydrologic Models, Water Resour. Res., 31(4), 995–1009, doi:10.1029/94WR02973, 1995.

EEA: CORINE Land Cover Project, [online] Available from: http://www.eea.europa.eu/publications/COR0-landcover, 1995.

Elder, K., Dozier, J. and Michaelsen, J.: Snow accumulation and distribution in an Alpine Watershed, Water Resour. Res., 27(7), 1541–1552, doi:10.1029/91WR00506, 1991.

Essery, R., Li, L. and Pomeroy, J.: A distributed model of blowing snow over complex terrain, Hydrol. Process., 13(14-15), 2423–2438, doi:10.1002/(SICI)1099-1085(199910)13:14/15<2423::AID-HYP853>3.0.CO;2-U, 1999.

Farinotti, D., Magnusson, J., Huss, M. and Bauder, A.: Snow accumulation distribution inferred from time-lapse photography and simple modelling, Hydrol. Process., 24(15), 2087–2097, doi:10.1002/hyp.7629, 2010.

Frey, S.: Possible Impacts of Climate Change on the Water Balance with Special Emphasis on Runoff and Hydropower Potential, University of Natural Resources and Life Sciences, Vienna. PhD thesis. [online] Available from: http://permalink.obvsg.at/AC10777542, 2015.

Fuchs, M.: Auswirkungen von möglichen Klimaänderungen auf die Hydrologie verschiedener Regionen in Österreich. (PhD thesis; in German)., University of Natural Resources and Life Sciences, Vienna., 2005.

Garvelmann, J., Pohl, S. and Weiler, M.: From observation to the quantification of snow processes with a time-lapse camera network, Hydrol. Earth Syst. Sci., 17(4), 1415–1429, doi:10.5194/hess-17-1415-2013, 2013.

Gharari, S., Hrachowitz, M., Fenicia, F., Gao, H. and Savenije, H. H. G.: Using expert knowledge to increase realism in environmental system models can dramatically reduce the need for calibration, Hydrol. Earth Syst. Sci., 18(12), 4839–4859, doi:10.5194/hess-18-4839-2014, 2014.

Gharari, S., Hrachowitz, M., Fenicia, F. and Savenije, H. H. G.: Moving beyond traditional model calibration or how to better identify realistic model parameters: sub-period calibration, Hydrol. Earth Syst. Sci. Discuss., 9(2), 1885–1918, doi:10.5194/hessd-9-1885-2012, 2012.

Gupta, H. V., Kling, H., Yilmaz, K. K. and Martinez, G. F.: Decomposition of the mean squared error and NSE performance criteria: Implications for improving hydrological modelling, J. Hydrol., 377(1-2), 80–91, doi:10.1016/j.jhydrol.2009.08.003, 2009.

Gupta, H. V., Wagener, T. and Liu, Y.: Reconciling theory with observations: elements of a diagnostic approach to model evaluation, Hydrol. Process., 22(18), 3802–3813, doi:10.1002/hyp.6989, 2008.

Haiden, T., Kann, A., Wittmann, C., Pistotnik, G., Bica, B. and Gruber, C.: The Integrated Nowcasting through Comprehensive Analysis (INCA) System and Its Validation over the Eastern Alpine Region, Weather Forecast., 26(2), 166–183, doi:10.1175/2010WAF2222451.1, 2011.

Hall, D. K., Riggs, G. A., Salomonson, V. V, DiGirolamo, N. E. and Bayr, K. J.: MODIS snow-cover products, Remote Sens. Environ., 83(1-2), 181–194, doi:10.1016/S0034-4257(02)00095-0, 2002.

Helfricht, K., Schöber, J., Schneider, K., Sailer, R. and Kuhn, M.: Interannual persistence of the seasonal snow cover in a glacierized catchment, J. Glaciol., 60(223), 889–904, doi:10.3189/2014JoG13J197, 2014.

Helfricht, K., Schöber, J., Seiser, B., Fischer, A., Stötter, J. and Kuhn, M.: Snow accumulation of a high alpine catchment derived from LiDAR measurements, Adv. Geosci., 32, 31–39, doi:10.5194/adgeo-32-31-2012, 2012.

Henriksen, H. J., Troldborg, L., Nyegaard, P., Sonnenborg, T. O., Refsgaard, J. C. and Madsen, B.: Methodology for construction, calibration and validation of a national hydrological model for Denmark, J. Hydrol., 280(1-4), 52–71, doi:10.1016/S0022-1694(03)00186-0, 2003.

Herrnegger, M., Nachtnebel, H.-P. and Haiden, T.: Evapotranspiration in high alpine catchments – an important part of the water balance!, Hydrol. Res., 43(4), 460, doi:10.2166/nh.2012.132, 2012.

Hiemstra, C. A., Liston, G. E. and Reiners, W. A.: Observing, modelling, and validating snow redistribution by wind in a Wyoming upper treeline landscape, Ecol. Modell., 197(1-2), 35–51, doi:10.1016/j.ecolmodel.2006.03.005, 2006.

Hock, R.: Temperature index melt modelling in mountain areas, J. Hydrol., 282(1-4), 104–115, doi:10.1016/S0022-1694(03)00257-9, 2003.

Holzmann, H., Lehmann, T., Formayer, H. and Haas, P.: Auswirkungen möglicher Klimaänderungen auf Hochwasser und Wasserhaushaltskomponenten ausgewählter Einzugsgebiete in Österreich (in german), Österreichische Wasser- und Abfallwirtschaft, 62(1-2), 7–14, doi:10.1007/s00506-009-0154-9, 2010.

Hrachowitz, M., Fovet, O., Ruiz, L., Euser, T., Gharari, S., Nijzink, R., Freer, J., Savenije, H. H. G. and Gascuel-Odoux, C.: Process consistency in models: The importance of system signatures, expert knowledge, and process complexity, Water Resour. Res., 50(9), 7445–7469, doi:10.1002/2014WR015484, 2014.

Huss, M., Bauder, A. and Funk, M.: Homogenization of long-term mass-balance time series, Ann. Glaciol., 50(50), 198–206, doi:10.3189/172756409787769627, 2009a.

Huss, M., Farinotti, D., Bauder, A. and Funk, M.: Modelling runoff from highly glacierized drainage basins in a changing climate, Mitteilungen der Versuchsanstalt fur Wasserbau, Hydrol. und Glaziologie an der Eidgenoss. Tech. Hochschule Zurich, 22(213), 123–146, doi:10.1002/hyp.7055, 2009b.

Jackson, T. H. R.: A Spatially Distributed Snowmelt-Driven Hydrologic Model applied to the Upper Sheep Creek Watershed. PhD thesis., Utah State University, Logan, Utah, USA., 1994.

Jonas, T., Marty, C. and Magnusson, J.: Estimating the snow water equivalent from snow depth measurements in the Swiss Alps, J. Hydrol., 378(1-2), 161–167, doi:10.1016/j.jhydrol.2009.09.021, 2009.

Kirchner, P. B., Bales, R. C., Molotch, N. P., Flanagan, J. and Guo, Q.: LiDAR measurement of seasonal snow accumulation along an elevation gradient in the southern Sierra Nevada, California, Hydrol. Earth Syst. Sci. Discuss., 11, 5327–5365, doi:10.5194/hessd-11-5327-2014, 2014.

Kling, H.: Spatio-Temporal Modelling of the Water Balance of Austria (PhD-thesis)., University of Natural Resources and Life Sciences, Vienna., 2006.

Kling, H., Fuchs, M. and Paulin, M.: Runoff conditions in the upper Danube basin under an ensemble of climate change scenarios, J. Hydrol., 424-425(0), 264–277, doi:10.1016/j.jhydrol.2012.01.011, 2012.

Kling, H., Fürst, J. and Nachtnebel, H. P.: Seasonal, spatially distributed modelling of accumulation and melting of snow for computing runoff in a long-term, large-basin water balance model, Hydrol. Process., 20(10), 2141–2156, doi:10.1002/hyp.6203, 2006.

Kling, H., Stanzel, P., Fuchs, M. and Nachtnebel, H.-P.: Performance of the COSERO precipitation-runoff model under non-stationary conditions in basins with different climates, Hydrol. Sci. J., 141217125340005, doi:10.1080/02626667.2014.959956, 2014a.

Kling, H., Stanzel, P. and Preishuber, M.: Impact modelling of water resources development and climate scenarios on Zambezi River discharge, J. Hydrol. Reg. Stud., 1, 17–43, doi:10.1016/j.ejrh.2014.05.002, 2014b.

Koboltschnig, G. R., Schöner, W., Zappa, M., Kroisleitner, C. and Holzmann, H.: Runoff modelling of the glacierized Alpine Upper Salzach basin (Austria): Multi-criteria result validation, in Hydrological Processes, vol. 22, pp. 3950–3964, John Wiley & Sons, Ltd., 2008.

Lehning, M., Bartelt, P., Brown, B., Fierz, C. and Satyawali, P.: A physical SNOWPACK model for the Swiss avalanche warning: part II. Snow microscrutcure, Cold Reg. Sci. Technol., 35(3), 147–167, doi:10.1016/S0165-232X(02)00073-3, 2002.

Lehning, M. and Fierz, C.: Assessment of snow transport in avalanche terrain, Cold Reg. Sci. Technol., 51(2-3), 240–252, doi:10.1016/j.coldregions.2007.05.012, 2008.

Liston, G. E.: Representing Subgrid Snow Cover Heterogeneities in Regional and Global Models, J. Clim., 17(6), 1381–1397, doi:10.1175/1520-0442(2004)017<1381:RSSCHI>2.0.CO;2, 2004.

Liston, G. E., Haehnel, R. B., Sturm, M., Hiemstra, C. a., Berezovskaya, S. and Tabler, R. D.: Simulating complex snow distributions in windy environments using SnowTran-3D, J. Glaciol., 53(181), 241–256, doi:10.3189/172756507782202865, 2007.

Liston, G. and Sturm, M.: A snow-transport model for complex terrain, J. Glaciol., 44(148), 1998.

Masson, V., Champeaux, J.-L., Chauvin, F., Meriguet, C. and Lacaze, R.: A Global Database of Land Surface Parameters at 1-km Resolution in Meteorological and Climate Models, J. Clim., 16(9), 1261–1282, doi:10.1175/1520-0442-16.9.1261, 2003.

Mauser, W. and Bach, H.: PROMET - Large scale distributed hydrological modelling to study the impact of climate change on the water flows of mountain watersheds, J. Hydrol., 376(3-4), 362–377, doi:10.1016/j.jhydrol.2009.07.046, 2009.

Melvold, K. and Skaugen, T.: Multiscale spatial variability of lidar-derived and modeled snow depth on Hardangervidda, Norway, Ann. Glaciol., 54(62), 273–281, doi:10.3189/2013AoG62A161, 2013.

Moore, R. J.: The PDM rainfall-runoff model, Hydrol. Earth Syst. Sci., 11(1), 483–499, doi:10.5194/hess-11-483-2007, 2007.

Nachtnebel, H. P., Baumung, S. and Lettl, W.: Abflussprognosemodell für das Einzugsgebiet der Enns und Steyer (in German), Vienna., 1993.

Nachtnebel, H. P., Senoner, T., Stanzel, P., Kahl, B., Hernegger, M., Haberl, U. and Pfaffenwimmer, T.: Inflow prediction system for the Hydropower Plant Gabčíkovo, Part 3 - Hydrologic Modelling, Bratislava., 2009.

Nikulin, G., Kjellström, E., Hansson, U., Strandberg, G. and Ullerstig, A.: Evaluation and future projections of temperature, precipitation and wind extremes over Europe in an ensemble of regional climate simulations, Tellus A, 63(1), 41–55, doi:10.1111/j.1600-0870.2010.00466.x, 2011.

Oubeidillah, A. A., Kao, S.-C., Ashfaq, M., Naz, B. S. and Tootle, G.: A large-scale, high-resolution hydrological model parameter data set for climate change impact assessment for the conterminous US, Hydrol. Earth Syst. Sci., 18(1), 67–84, doi:10.5194/hess-18-67-2014, 2014.

Pohl, S., Garvelmann, J., Wawerla, J. and Weiler, M.: Potential of a low-cost sensor network to understand the spatial and temporal dynamics of a mountain snow cover, Water Resour. Res., 50(3), 2533–2550, doi:10.1002/2013WR014594, 2014.

Pomeroy, J. W., Gray, D. M., Hedstrom, N. R. and Janowicz, J. R.: Prediction of seasonal snow accumulation in cold climate forests, Hydrol. Process., 16(18), 3543–3558, doi:10.1002/hyp.1228, 2002.

Pomeroy, J. W., Gray, D. M., Shook, K. R., Toth, B., Essery, R. L. H., Pietroniro, A. and Hedstrom, N.: An evaluation of snow accumulation and ablation processes for land surface modelling, Hydrol. Process., 12(15), 2339–2367, doi:10.1002/(SICI)1099-1085(199812)12:15<2339::AID-HYP800>3.0.CO;2-L, 1998.

Prasad, R., Tarboton, D. G., Liston, G. E., Luce, C. H. and Seyfried, M. S.: Testing a blowing snow model against distributed snow measurements at Upper Sheep Creek, Idaho, United States of America, Water Resour. Res., 37(5), 1341–1356, doi:10.1029/2000WR900317, 2001.

Rasmussen, R. M., Hallett, J., Purcell, R., Landolt, S. D. and Cole, J.: The hotplate precipitation gauge, J. Atmos. Ocean. Technol., 28, 148–164, doi:10.1175/2010JTECHA1375.1, 2011.

Riley, J., Israelsen, E. and Eggleston, K.: Some approaches to snowmelt prediction, Role Snowmelt Ice Hydrol. IAHS Publ. 107, 956–971, 1973.

Rosenbrock, H.: An automatic method for finding the greatest or least value of a function, Comput. J., 3(3), 175–184, doi:10.1093/comjnl/3.3.175, 1960.

Rutter, N., Essery, R., Pomeroy, J., Altimir, N., Andreadis, K., Baker, I., Barr, A., Bartlett, P., Boone, A., Deng, H., Douville, H., Dutra, E., Elder, K., Ellis, C., Feng, X., Gelfan, A., Goodbody, A., Gusev, Y., Gustafsson, D., Hellström, R., Hirabayashi, Y., Hirota, T., Jonas, T., Koren, V., Kuragina, A., Lettenmaier, D., Li, W. P., Luce, C., Martin, E., Nasonova, O., Pumpanen, J., Pyles, R. D., Samuelsson, P., Sandells, M., Schädler, G., Shmakin, A., Smirnova, T. G., Stähli, M., Stöckli, R., Strasser, U., Su, H., Suzuki, K., Takata, K., Tanaka, K., Thompson, E., Vesala, T., Viterbo, P., Wiltshire, A., Xia, K., Xue, Y. and Yamazaki, T.: Evaluation of forest snow processes models (SnowMIP2), J. Geophys. Res. Atmos., 114, doi:10.1029/2008JD011063, 2009.

Safeeq, M., Mauger, G. S., Grant, G. E., Arismendi, I., Hamlet, A. F. and Lee, S.-Y.: Comparing Large-Scale Hydrological Model Predictions with Observed Streamflow in the Pacific Northwest: Effects of Climate and Groundwater*, J. Hydrometeorol., 15(6), 2501–2521, doi:10.1175/JHM-D-13-0198.1, 2014.

Schaefli, B., Hingray, B., Niggli, M. and Musy, A.: A conceptual glacio-hydrological model for high mountainous catchments, Hydrol. Earth Syst. Sci., 9(1/2), 95–109, doi:10.5194/hess-9-95-2005, 2005.

Schöber, J., Schneider, K., Helfricht, K., Schattan, P., Achleitner, S., Schöberl, F. and Kirnbauer, R.: Snow cover characteristics in a glacierized catchment in the Tyrolean Alps - Improved spatially distributed modelling by usage of Lidar data, J. Hydrol., 519, 3492–3510, doi:10.1016/j.jhydrol.2013.12.054, 2014.

Scipión, D. E., Mott, R., Lehning, M., Schneebeli, M. and Berne, A.: Seasonal small-scale spatial variability in alpine snowfall and snow accumulation, Water Resour. Res., 49, 1446–1457, doi:10.1002/wrcr.20135, 2013.

Shulski, M. D. and Seeley, M. W.: Application of Snowfall and Wind Statistics to Snow Transport Modeling for Snowdrift Control in Minnesota, J. Appl. Meteorol., 43(11), 1711–1721, doi:10.1175/JAM2140.1, 2004.

Sovilla, B., Mcelwaine, J. N., Schaer, M. and Vallet, J.: Variation of deposition depth with slope angle in snow avalanches: Measurements from Vallée de la Sionne., 2010.

Stanzel, P., Kahl, B., Haberl, U., Herrnegger, M. and Nachtnebel, H. P.: Continuous hydrological modelling in the context of real time flood forecasting in alpine Danube tributary catchments, IOP Conf. Ser. Earth Environ. Sci., 4, 012005, doi:10.1088/1755-1307/4/1/012005, 2008.

Stanzel, P. and Nachtnebel, H. P.: Mögliche Auswirkungen des Klimawandels auf den Wasserhaushalt und die Wasserkraftnutzung in Österreich (in German), Österreichische Wasser- und Abfallwirtschaft, 62(9-10), 180–187, doi:10.1007/s00506-010-0234-x, 2010.

Strasser, U., Bernhardt, M., Weber, M., Liston, G. E. and Mauser, W.: Is snow sublimation important in the alpine water balance?, Cryosph., 2, 53–66, doi:10.5194/tc-2-53-2008, 2008.

Thornthwaite, C. W.: An Approach toward a Rational Classification of Climate, Geogr. Rev., 38(1), 55–94, 1948.

Weber, M., Braun, L., Mauser, W. and Prasch, W.: Contribution of rain, snow- and icemelt in the upper Danube discharge today and in the future, Geogr. Fis. e Din. Quat., 33(2), 221–230, 2010.

Williams, M. W., Bardsley, T. and Rikkers, M.: Overestimation of snow depth and inorganic nitrogen wetfall using NADP data, Niwot Ridge, Colorado, Atmos. Environ., 32, 3827–3833, doi:10.1016/S1352-2310(98)00009-0, 1998.

Winstral, A., Elder, K. and Davis, R. E.: Spatial Snow Modeling of Wind-Redistributed Snow Using Terrain-Based Parameters, J. Hydrometeorol., 3(5), 524–538, doi:10.1175/1525-7541(2002)003<0524:SSMOWR>2.0.CO;2, 2002.

Wood, E. F., Lettenmaier, D. P. and Zartarian, V. G.: A land-surface hydrology parameterization with subgrid variability for general circulation models, J. Geophys. Res., 97(D3), 2717, doi:10.1029/91JD01786, 1992.

Table 1. Land use classes used in COSERO (derived from CORINE land cover data, EEA, 1995) and their proportion in the Ötztal. Snow holding capacities H_v for each type of land use are taken from (Liston and Sturm, 1998; Prasad et al., 2001).

Land use class	proportion [%]	Snow holding capacity H_v [mm]
Build-up areas	1.2	100
Pastures and meadows	20.9	500
Coniferous forests	8.1	2500
Sparsely vegetated areas	20.9	300
Bare rocks	29.5	200
Glaciers	19.4	200

Table 2. Comparison of performances of model A and B with respect to snow cover and runoff. For snow cover coefficient of determination (R^2) was used, whereas Kling-Gupta-Efficiency (Gupta et al., 2009) was used for runoff.

	Calibration		Validation	
	Snow cover (R^2)	Runoff (KGE)	Snow cover (R^2)	Runoff (KGE)
MODEL A	0.78	0.93	0.74	0.92
MODEL B	0.70	0.88	0.66	0.90

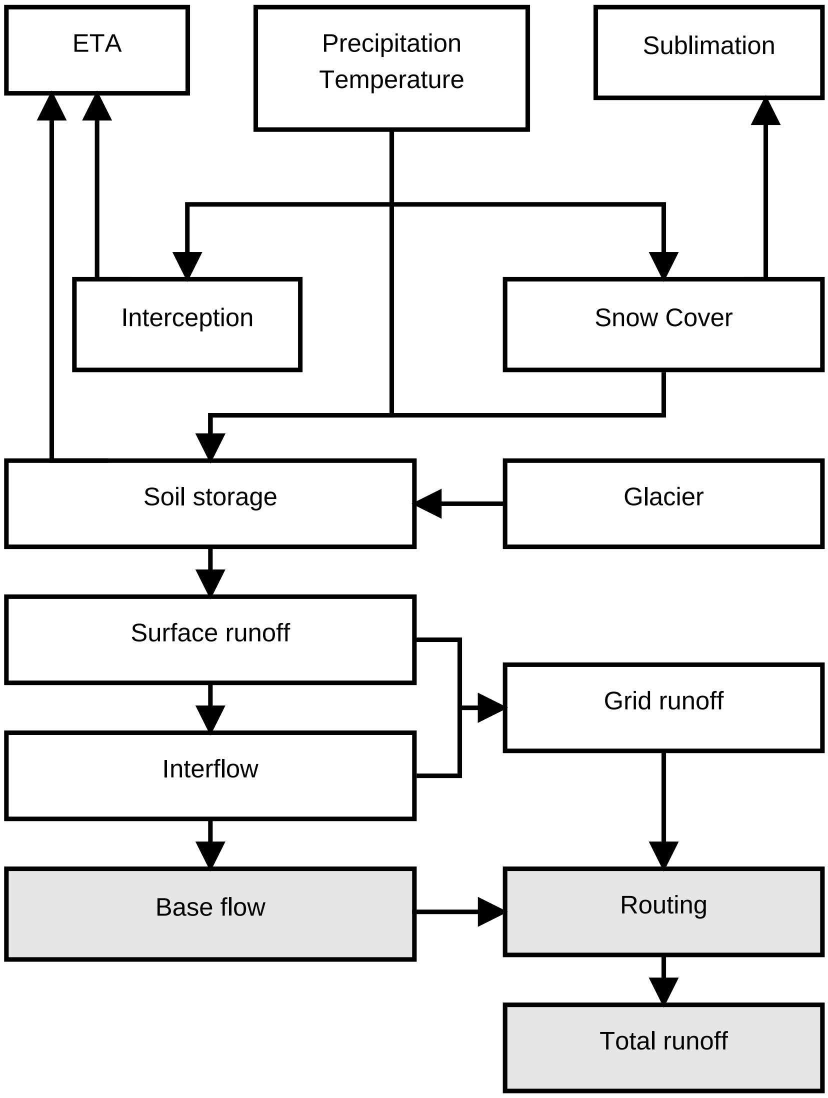

Figure 1. Flow chart of the conceptual model COSERO. Potential evapotranspiration is estimated using the Thornthwaite method (Thornthwaite, 1948). White parts represent distributed processes, greyish parts are calculated on a subbasin scale. Snow transport is implemented in the snow cover module.

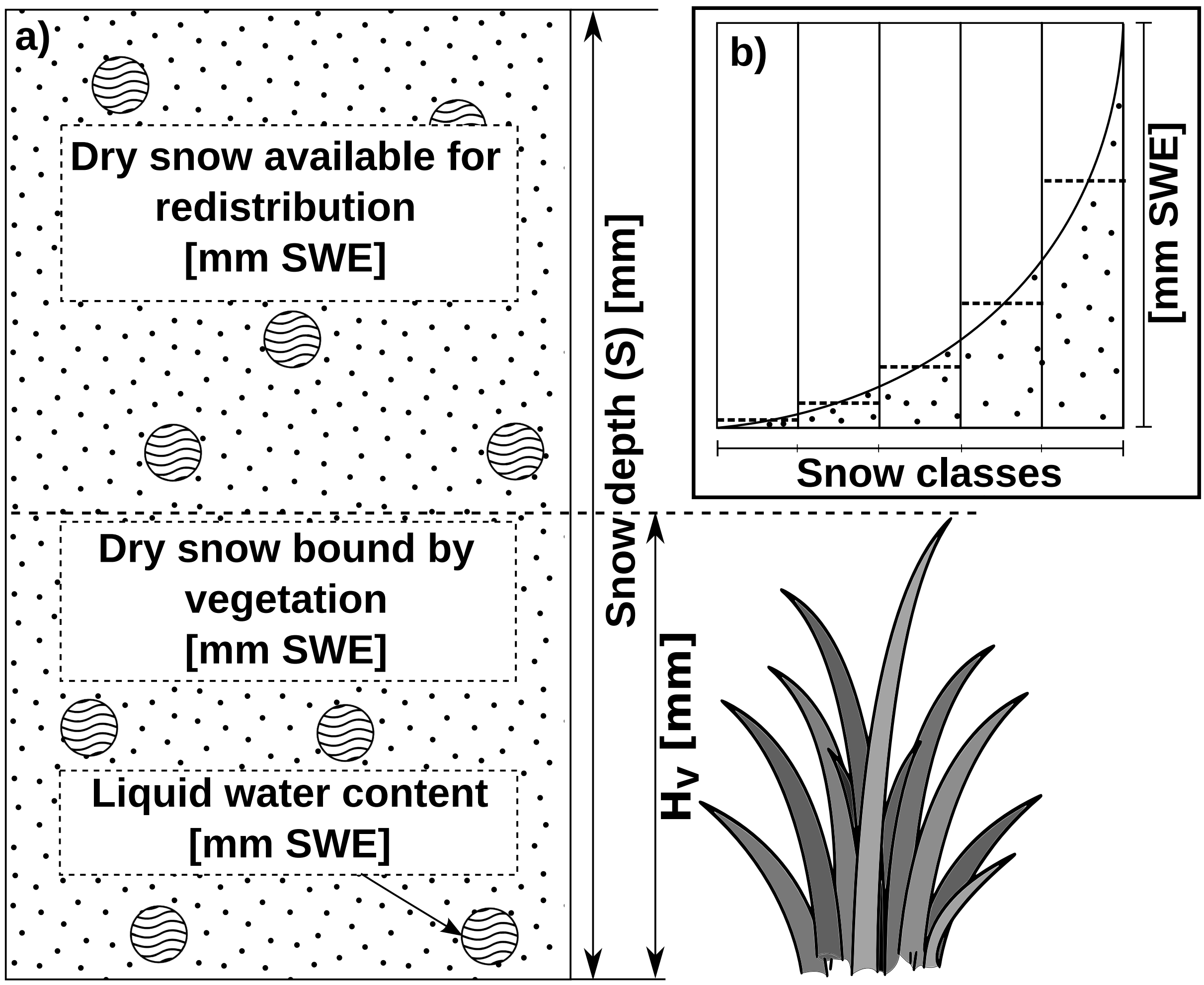

Figure 2. Schematic view of the snow cover in COSERO. a) Composition of one snow class. Vegetation or surface roughness defines the threshold value (H_V) to hold back an amount of snow. b) View of one grid cell including five snow classes each of which is composed in the way shown in a). Snowfall is distributed log-normally throughout the classes (dashed lines in b)). Note that snow depth S is given in mm while all other parameters regarding snow are given in mm SWE.

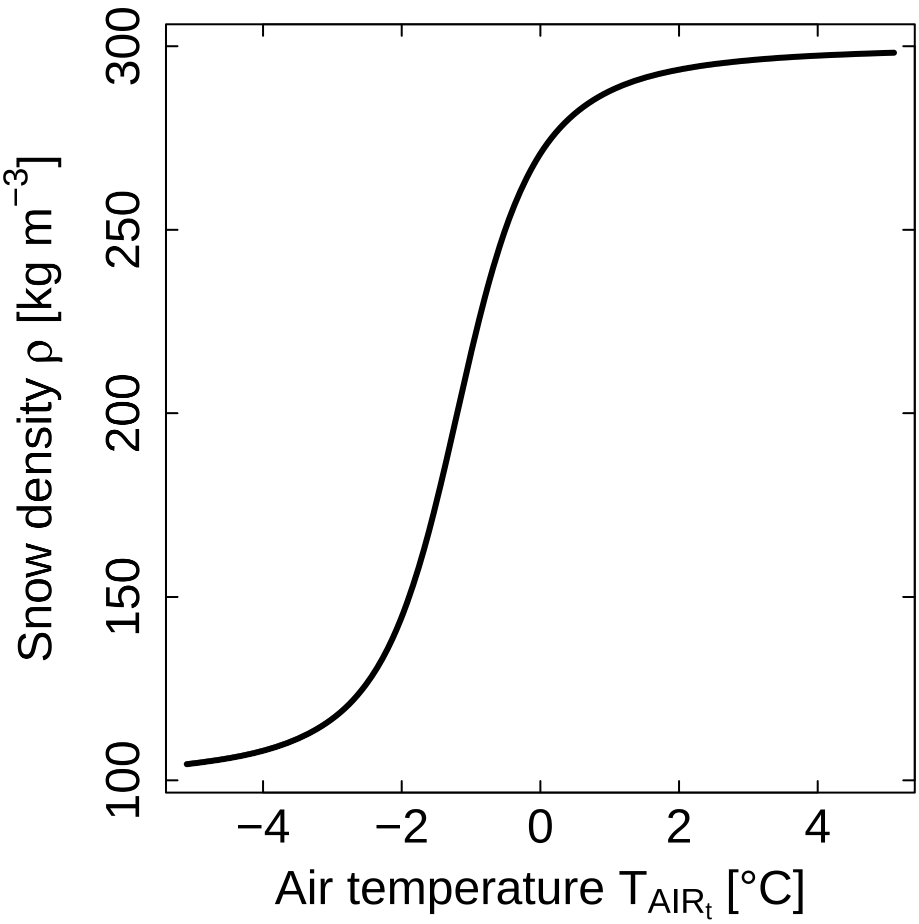

Figure 3. Estimation of the density of snow using Eqs. (8) and (9). Minimum and maximum densities of fresh snow are 100 and 300 kg m^{-3}, respectively.

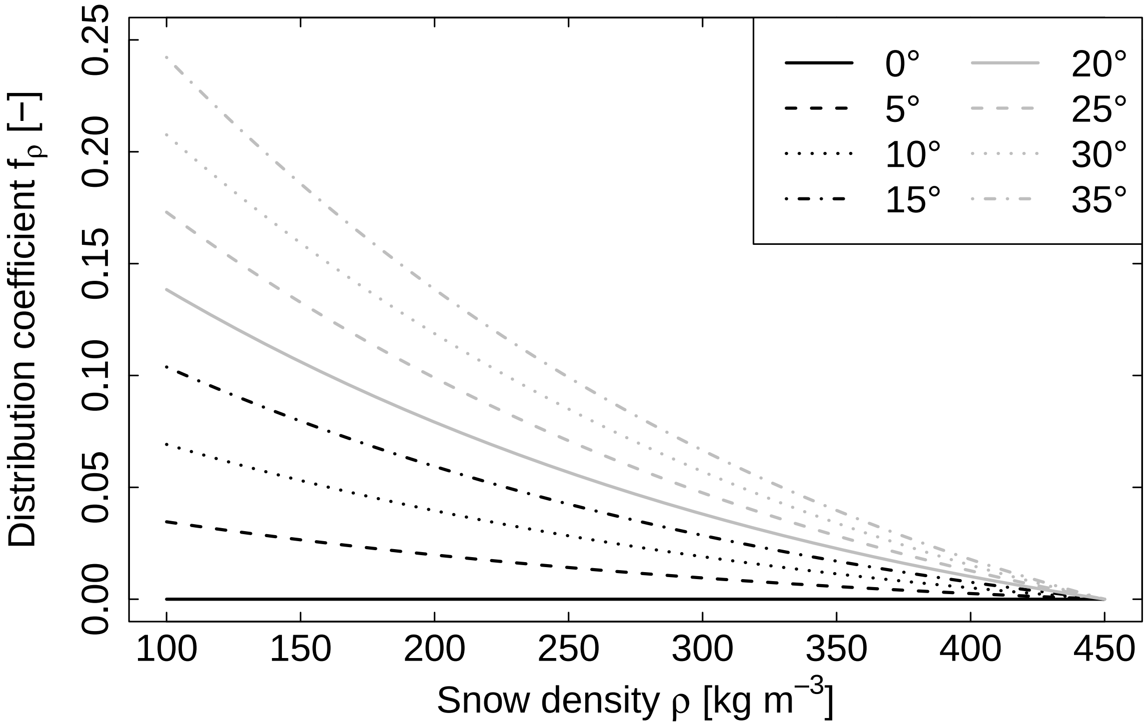

Figure 4. Shapes of the distribution coefficient in dependency of different slope angles and snow densities. If cold snow with a density of 100 kg m^{-3} is located on a slope of 35°, a portion of 25% of the available snow is transported to the neighbour cell. If the snow density reaches its maximum value, no transport occurs regardless of the slope.

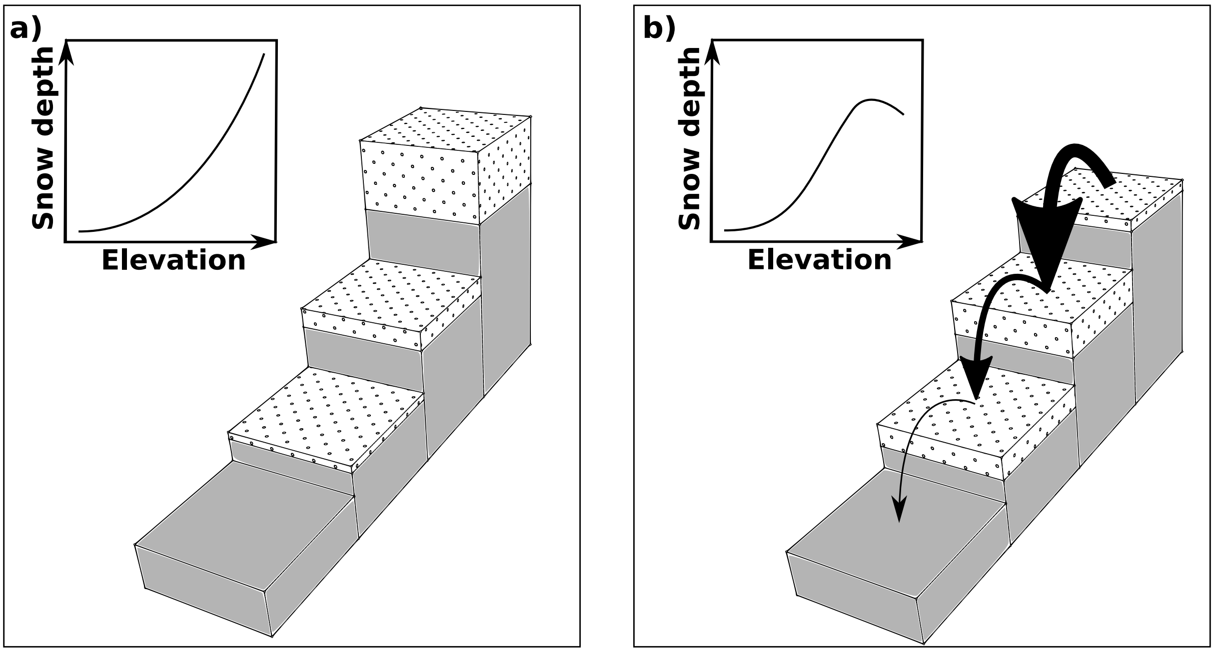

Figure 5. Conceptual snow accumulations in mountainous regions without (a) and with (b) considering lateral snow transport processes. Dotted blocks represent exaggerated snow accumulations. Applying the redistribution model snow is transported from the highest grid cell to its neighbour where it is treated like solid precipitation. From this grid cell a portion of snow gets transported to the downward neighbour again and so forth until either the terrain is too flat or snow depths do not exceed the threshold for vegetation (see Fig. 4). Consequently less snow remains in the summit region whereas lower grid cells show enhanced accumulation. Although snow depths in the summits are lower, the amount of snow covered cells stay similar as some residual snow remains in all cells due to H_V parameterization.

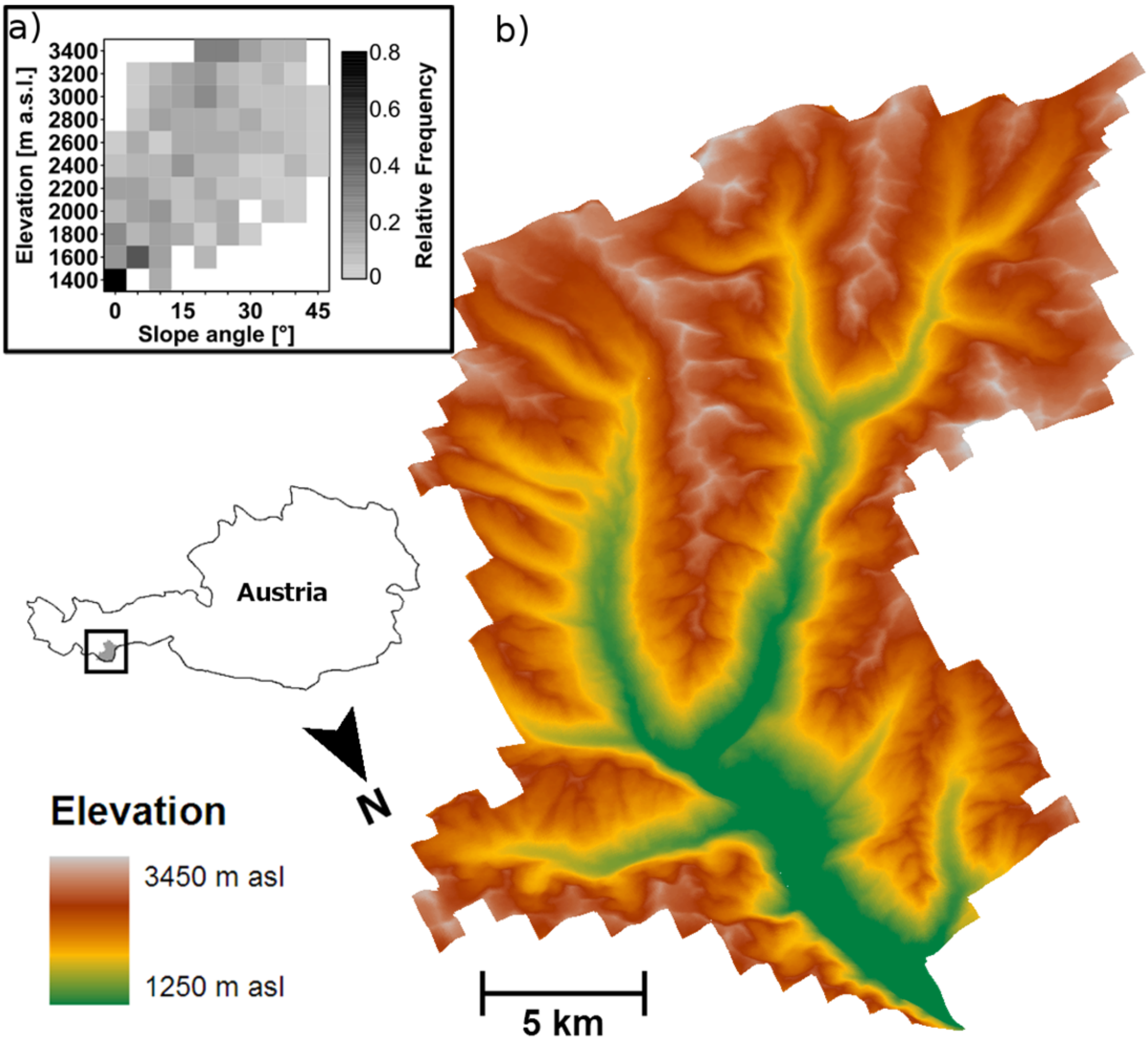

Figure 6. Elevation levels of the Ötztal using a 1x1 km grid (b). Frequency distribution of slope angles derived from 1x1 km grid are shown (a). Slopes in general are steeper in the summit regions than in the valleys. Note that instead of the average slope of a grid cell only steepest vertical gradients are plotted.

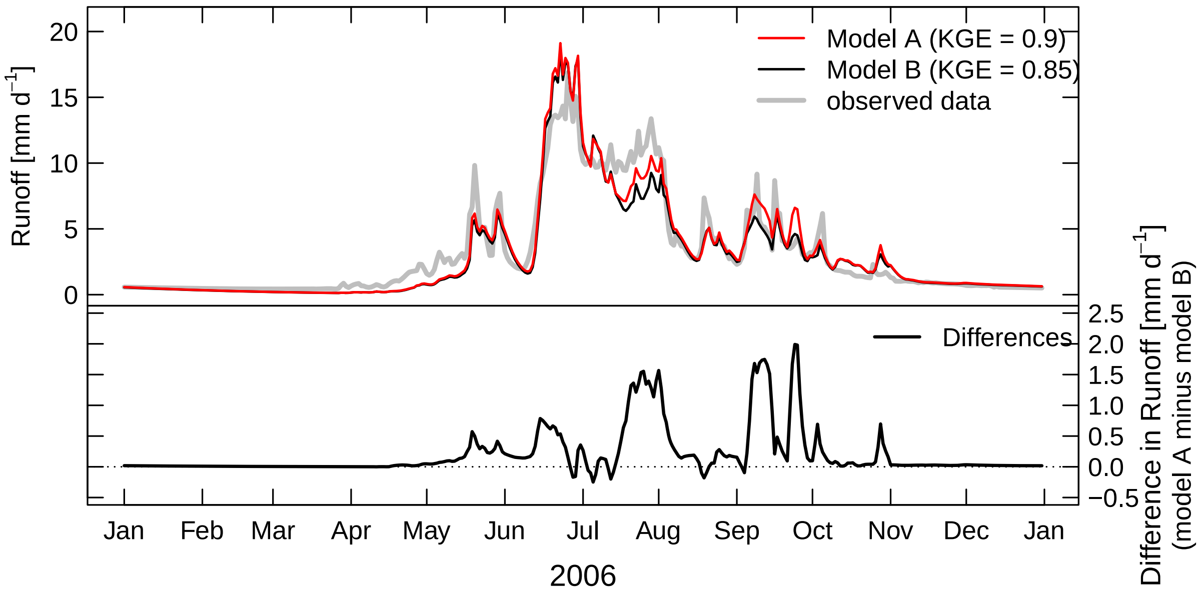

Figure 7. Specific runoff at the outlet at Huben is modelled with (model A) and without (model B) using the snow redistribution routine. In the early snow melt period, more runoff is generated by model A because snow accumulates rather in lower than in higher levels. In summer, enhanced glacier melt leads to more runoff by model A.

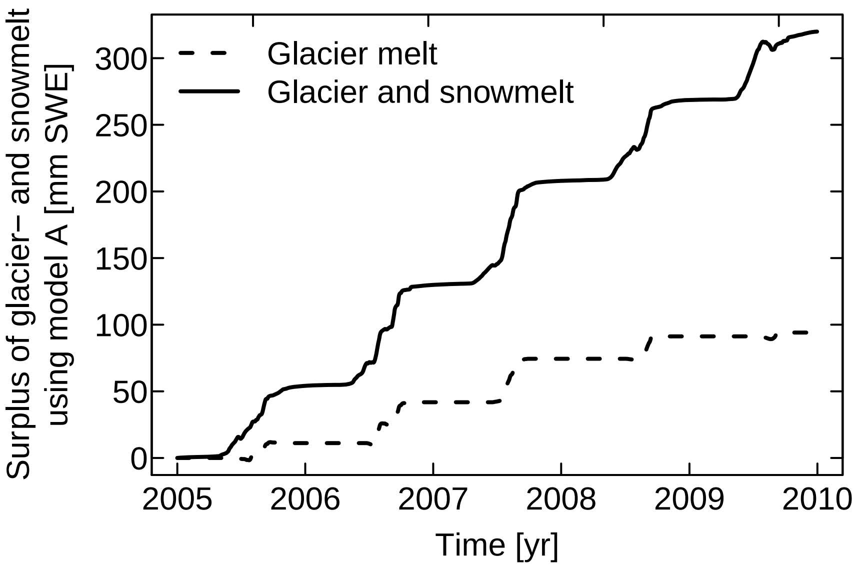

Figure 8. Accumulated differences (model A minus model B) in discharge at gauge Huben. Using model B, about 300 mm SWE in five years are remaining in the catchment due to snow accumulation processes and less glacier melt.

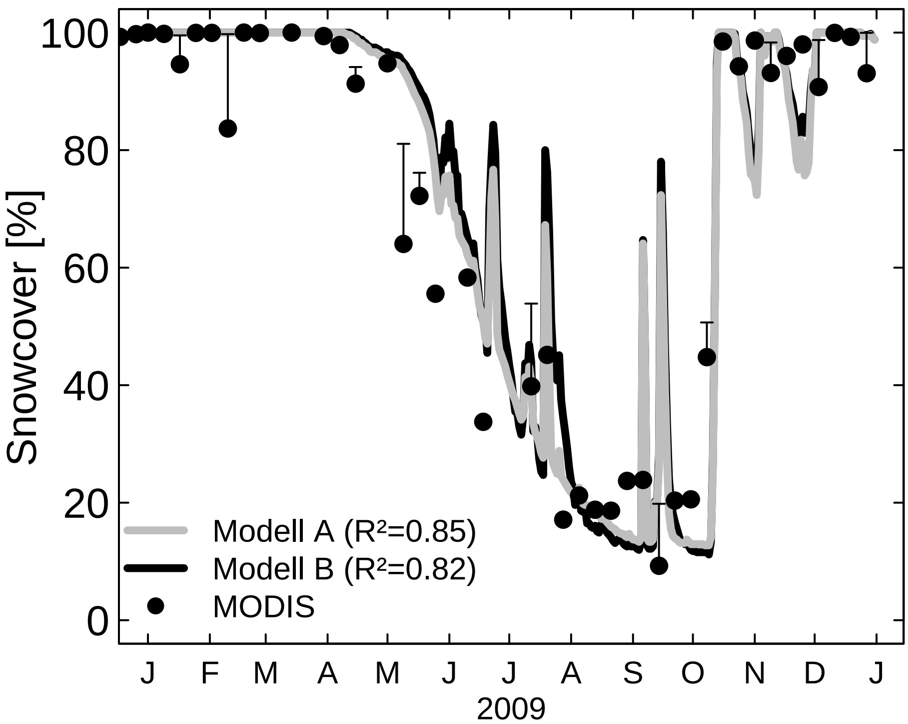

Figure 9. Snow cover in 2009 modelled by both model A and B compared with MODIS data. Error bars refer to uncertainties due to cloud coverage.

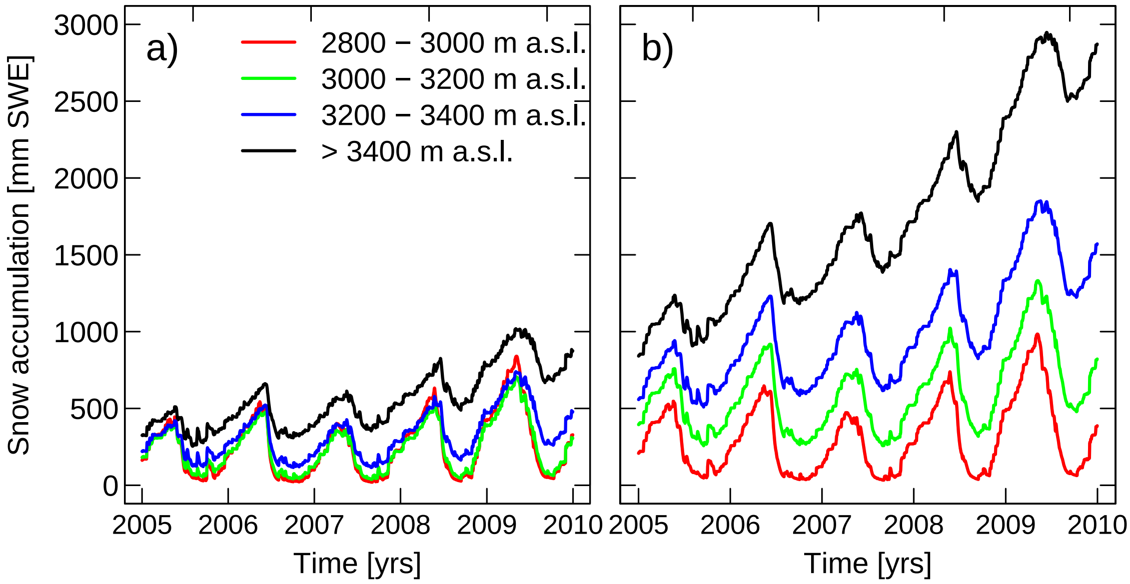

Figure 10. Behaviour of snow accumulation and melt of model A (a) and B (b) in the upper elevations. Model B leads to “snow towers” of approx. 2900 mm SWE in regions above 3400 m a.s.l. in seven years of modelling, whereas model A does not show such behaviour. In elevations lower 2800 m a.s.l. neither model A nor B show accumulation behaviour. Note that model results are shown from 2005 to 2010 without the warm-up period for clarity reasons. Therefore snow depth does not start at zero in the figure while it does at the beginning of the modelling.

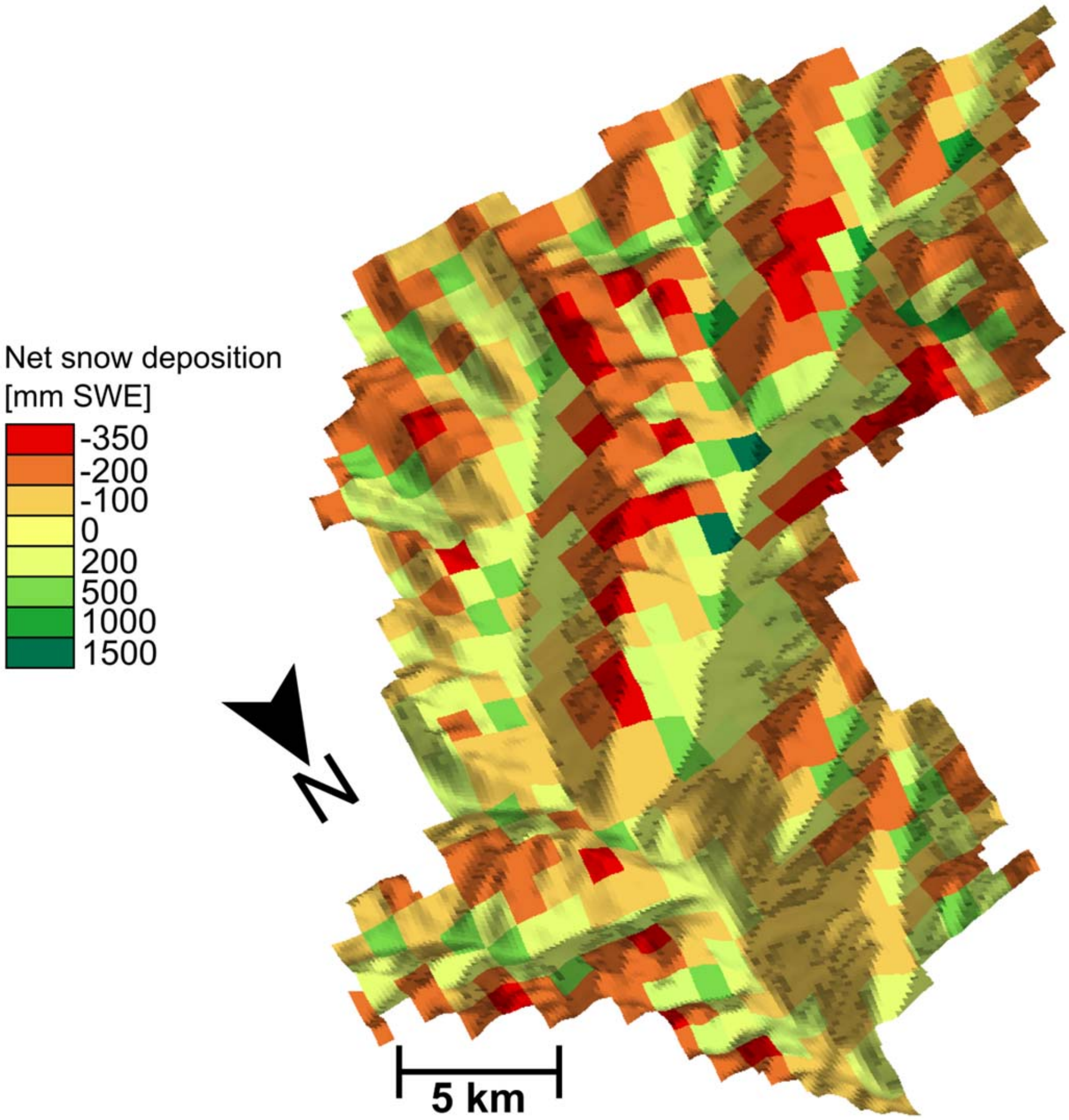

Figure 11. Net snow deposition in the catchment during the time period of one year. Negative values refer to a net loss, positive to a net gain of snow. Raster cells in the peak regions act as donor cells and do not receive any snow whereas mean elevated cells may act as donor and acceptor in the same time. Note that, since only the net deposition of snow based on lateral transport is shown, values cannot be linked to snow depths at the end of the time period.